UNIVERSITÀ
DEGLI STUDI
DI UDINE

Università degli studi di Udine

Automatic MTPA Tracking in IPMSM Drives: Loop Dynamics, Design, and Auto-Tuning

Original

Availability:
This version is available http://hdl.handle.net/11390/1127911 since 2020-03-05T10:37:50Z

Publisher:

Published
DOI:10.1109/TIA.2017.2708683

Terms of use:
The institutional repository of the University of Udine (http://air.uniud.it) is provided by ARIC services. The aim is to enable open access to all the world.

Publisher copyright

(Article begins on next page)

19 April 2024

Automatic MTPA Tracking in IPMSM Drives: Loop Dynamics, Design and Auto-Tuning

Nicola BEDETTI
Drives and Motion Control Unit (DMCU)
Gefran, s.p.a.
Gerenzano, Varese, ITALY
nicola.bedetti@gefran.com

Sandro CALLIGARO, Christian OLSEN, Roberto PETRELLA
Polytechnic Department of Engineering and Architecture (DPIA)
University of Udine
Udine, ITALY
sandro.calligaro@uniud.it, edlab@uniud.it, roberto.petrella@uniud.it

***Abstract*—Maximum Torque Per Ampere (MTPA) based on motor parameters is a common approach to achieve high efficiency and torque density in Interior Permanent Magnet Synchronous Machines (IPMSMs) drives. However, uncertainty (e.g. due to identification errors, magnetic saturation or temperature variation) results in undesired deviation from the optimal operating trajectory. To solve this problem, MTPA tracking methods have been proposed, which exploit signal injection to search the minimum current point for a certain load torque, in a closed-loop fashion. Closed-form design of the MTPA tracking loop dynamics has never been addressed in past literature and represents the main topic of this paper. A recent and efficient tracking method has been considered for the analysis and case study, i.e. [14]. Non-linear small signal gain of the loop can be calculated in closed form, leading to two valuable results: dynamics can be programmed by optimal design of the tracking regulator; on-line adaptation can be applied, making the designed MTPA tracking dynamics invariant with the operating point. A straightforward and effective solution is proposed for the regulator design, which allows to obtain the desired bandwidth and first order tracking response in the whole range of operation, being also suitable for auto tuning and on-line adaptation.**

The proposed method has been studied analytically and in simulation, also considering the influence of noise and parametric uncertainties. Finally the technique has been implemented on the hardware of a commercial industrial drive, proving the effectiveness of the proposal. The proposed concepts described in this paper, design approach and adaptation strategy, analyzed here for the first time, are general and can be applied to any control scheme implementing closed-loop MTPA tracking.

Keywords—MTPA tracking; linearization; auto-tuning; MTPA loop dynamics; adaptive control; IPMSM drive; extremum seeking.

LIST OF SYMBOLS

L_d, L_q	direct- and quadrature-axis inductance
Λ_{mg}	permanent-magnet flux-linkage
pp	pole-pairs
T_e, T_0	electromechanical torque (actual value and equilibrium point)
i_d, i_q	direct- and quadrature-axis current
i_{dq}	stator current space vector
i_s,i_{s_0}, δi_s	current space vector "magnitude with torque sign" (actual value, equilibrium point, small-signal variation)
$\gamma, \gamma_0, \delta\gamma, \gamma_{MTPA}$	current space vector phase (actual value, equilibrium point, small-signal variation and MTPA value)
f_i	signal injection frequency
A	signal injection amplitude
k_{HPF}	high-pass filtering equivalent gain
f_{HPF}	high-pass filter pole frequency
$C(s), P(s)$	transfer functions of speed controller and mechanical plant
$W(s)$	current space vector magnitude vs. phase angle small-signal transfer function
ϵ_f	MTPA tracking error signal
Ω_{loop}	speed control closed-loop transfer function
g	small-signal gain of the tracking loop
$K_{i_{MTPA}}$	MTPA tracking regulator integral gain
B_{MTPA}	desired tracking bandwidth
V	Lyapunov candidate function
$\|\ \|$	vector magnitude
*	control reference value
$\widehat{\ }$	estimated variable
$LPF\{\ \}$	low-pass filtering
$\Re e\{\ \}$	complex variable real part
$\angle\{\ \}$	complex variable argument

I. INTRODUCTION

Interior Permanent Magnet Synchronous Machines drives are usually adopted in applications where efficiency and power density are crucial. Maximum Torque Per Ampere trajectory is a common approach to the maximization of these figures of merit below the base speed. The MTPA curve, which is usually expressed in the dq currents plane (i.e. rotor-synchronous currents, direct-, d, and quadrature-axis, q), depends on the magnetic motor parameters, namely apparent inductances and permanent magnet flux-linkage. Conventional MTPA implementation consist in the on-line calculation of synchronous reference frame currents, based on rated machine parameters and torque request. Differentiation of the machine torque equation with respect to the stator current provides in fact closed-form formulas which are well known, [1], and are widely used in many drive systems. Unfortunately, knowledge of machine parameters is often uncertain (e.g. due to identification errors, especially if self-identification is adopted) and variation can occur during operation due to magnetic saturation or changes in temperature. Parametric errors result in deviation from the optimal operating point loci, which finally leads to additional losses and/or decreased torque density. In order to overcome this issue, various on-line approaches have been proposed in recent years, mainly based on parameters estimation, [1]-[7], or dynamic tracking of the MTPA condition, [8]-[14][17].

The first class of methods is based on the on-line estimation of machine parameters and real-time adaptation of the reference current trajectory based on estimated values and analytical formulas, [1]-[3]. Conventional MTPA control schemes are normally adopted, where the estimated parameters are considered, instead of the rated ones, for the calculation of the optimal trajectory. The complexity of such methods is quite high due to the need of estimating many parameters on-line. Moreover, the accuracy of estimates strongly affects that of the MTPA operating point. Finally, the number of estimated parameters is limited, e.g. quadrature inductances and PM flux linkage, while cross-saturation effects are normally not considered, leading to a poor overall accuracy of the MTPA trajectory. Very recent parameter identification proposals, [5]-[7], allow a relatively accurate estimation of machine parameters at stand-still and can be effectively employed for the self-tuning of the drive parameters, including the MTPA generation engine. However, also in this case slow variations that could occur during normal drive operation, e.g. due to temperature or aging, are not taken into account and require a different approach.

Dynamic tracking techniques for the MTPA locus have been proposed relatively recently, [8]-[14][17], and are aimed at estimating the optimal operating point, i.e. finding out the current vector angle that minimizes the current magnitude for a certain steady-state load torque, by applying an on-line modification of the reference current space vector and adaptation based on machine response to such a stimulus. In this case accuracy can be ensured independent of machine parameters, differently from other approaches.

Some techniques of this kind are based on a slow modification of current space vector phase angle, searching for the value which provides the minimum of stator current at a given load torque, [8]. The main drawback of such methods is related to their dynamical performance, which has to be necessarily slow in order to ensure robustness during machine transients. Moreover, according to this approach, the current vector angle needs to be changed even at steady-state, thus introducing additional noise and reducing the overall efficiency of the system. Stability issues and convergence time of such methods have not been addressed.

More interesting approaches are based on the superposition of a small pulsating current component to the fundamental one, in order to seek and adapt on-line the MTPA during normal operation of the drive, [9]-[14][17]. They are mainly based on the minimization of torque oscillations due to the injected current, this last condition corresponding to MTPA operation. The type of the performed injection (e.g. high-frequency phase angle oscillation or pulsating current space vector along a certain direction), and the algorithm used for the extraction of the information needed to adapt the operating point is quite similar among these methods, even though interesting differences exist. Some of these techniques require high-accuracy speed measurement for a proper detection of out-of-MTPA conditions, which represents a heavy limitation of the accuracy and bandwidth of the estimation algorithm, [9]. Moreover, a larger than usual bandwidth needs to be achieved by the current control loop, for optimal operation of the tracking algorithm, [10][11]. The performance and reliability of this class of methods is finally demonstrated for both Synchronous Reluctance Machines (SynRM) and IPMSM, [12][13], even in the case of magnetic saturation.

A recent interesting proposal, [14], considers the injection of a small sinusoidal perturbation of the current space vector phase angle, seeking for null derivative of the current amplitude at constant torque, i.e. the MTPA condition by definition. An important contribution in this case is the analytical description of the non-linear tracking loop dynamics, in order to address stability and to provide an upper bound estimation of the convergence time as a function of the starting point. Unfortunately, the analysis shows that the small-signal dynamics varies as a function of the operating condition and an explicit criterion for the design of the MTPA tracking regulator is not provided.

This paper extends the analysis proposed in [14] by introducing a method for the approximation of the MTPA tracking loop dynamics, [17]. This leads to a simplified equivalent small-signal linearized system. Using the relatively simple expression of the small-signal gain, it becomes possible to apply on-line adaptation of the tracking regulator in order to normalize the loop transfer function, making the MTPA tracking dynamics invariant with the operating point. By using this approach, analytical design methods for the regulator become straightforward. In particular a simple design method is proposed, which aims at obtaining a first-order closed-loop response with a certain bandwidth, which is kept constant in the whole operating range. Given its simplicity, this design procedure is suitable for auto-tuning and at the same time the computational burden related to on-line adaptation is acceptable in a typical modern drive control system. Some properties of the algorithm will also be investigated, with particular attention to implementation issues, such as the requirements for the current and speed controllers, which are involved in the MTPA estimation loop dynamics. It is worth noticing that the proposed ideas, design approach and adaptation strategy are indeed general and can be

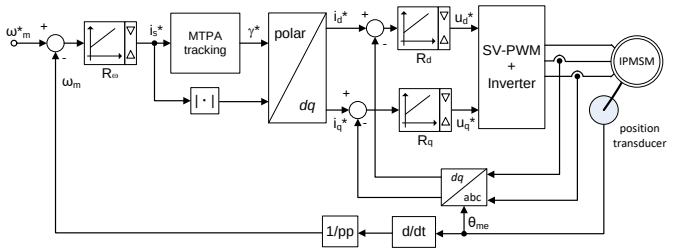

Fig. 1. Speed regulation with MTPA tracking implementation.

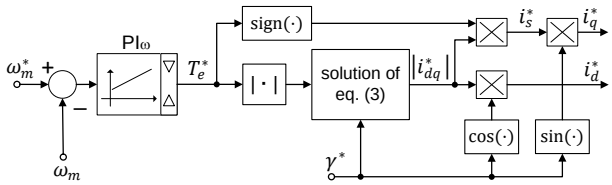

Fig. 2. Control scheme adopting torque reference and arbitrary current angle.

applied to any control scheme implementing closed-loop MTPA tracking, e.g. [9][11][13].

In the following two sections, some preliminary concepts will be recalled, comprising the definition of the MTPA problem and its solution by means of the MTPA tracking loop based on extremum seeking. Then, the results of the study on the dynamics already present in literature will be resumed, and finally the proposed study will be presented, in which proper approximations are introduced, leading to a simpler dynamical analysis. Thanks to an on-line adaptation technique, the tracking loop regulator can be easily designed in order to ensure stability and obtain predictable bandwidth. The proposed technique has been first analyzed from a theoretical point of view. A simulation model of the complete system has then been implemented to provide a preliminary validation of the analytical results. Finally, experimental tests show a very good agreement with theoretical results, confirming the effectiveness of the proposal and the feasibility of implementation on a typical industrial drive architecture.

II. MTPA TRACKING FORMULATION

The analytical expression of the electromechanical torque in an interior permanent magnet synchronous machine is:

$$T_e = \frac{3}{2} pp \ \left[\Lambda_{mg} i_q + \left(L_d - L_q\right) i_d i_q\right] \tag{1}$$

where pp is the number of pole pairs, Λ_{mg} is the permanent magnet flux-linkage magnitude, and L_d, L_q are the direct and quadrature-axis (apparent) inductances, respectively. If current space vector is expressed in polar coordinates, i.e. considering its magnitude $|i_{dq}|$ and phase γ,

$$i_d = |i_{dq}| \cdot \cos(\gamma) \quad , \quad i_q = |i_{dq}| \cdot \sin(\gamma) \tag{2}$$

equation (1) can be rewritten as

$$T_e = \frac{3}{2} pp \ \left[\Lambda_{mg} |i_{dq}| \sin\gamma + \left(L_d - L_q\right) |i_{dq}|^2 \sin\gamma \cos\gamma\right] \tag{3}$$

In this paper, as well as in other papers dealing with MTPA tracking, [9]-[11][14], a common IPMSM speed control scheme is considered (Fig. 1), in which a speed regulator provides a torque-related reference signal i_s^*, which has the physical meaning of the reference current space vector "magnitude with torque sign":

$$i_d^* = |i_s^*| \cdot cos(\gamma^*) \quad , \quad i_q^* = |i_s^*| \cdot sin(\gamma^*) \tag{4}$$

However, a speed regulator with actual torque reference output can also be sketched, as shown in Fig. 2. Inversion of torque equation (3) has been considered in order to calculate the magnitude of the reference current space vector as a function of the required torque.

The underlying peculiarity of both the control schemes is that the current reference vector angle γ^* can be set arbitrarily. This angle is usually chosen in order to approximate the MTPA trajectory by means of a Look-Up Table (LUT) or approximating function. In the case considered in this paper, as it will be shown in the following, the angle reference is generated by an MTPA tracking algorithm. It is also worth mentioning that this kind of control schemes are particularly suitable to the implementation of Flux-Weakening (F-W) algorithms, both with feed-forward, [15], or feed-back methods, [16]. As reported in previous literature, smooth transition between MTPA and F-W is achieved by proper saturation of the voltage regulator, [16]. The solution based on torque reference (Fig. 2) also provides an additional advantage, i.e. the linearity of the speed control is maintained, independent of the value of the reference angle γ^*.

For the sake of simplicity, in the following study the control scheme in Fig. 1 will be considered, and only the positive torque case will be taken into account, since the torque production properties of the machine are symmetrical with respect to the d-axis, i.e.

$$T_e\left(i_d, +i_q\right) = -T_e\left(i_d, -i_q\right) \tag{5}$$

This allows to restrict the analysis to the range

$$\gamma^* \epsilon \, [\pi/2, \pi] \tag{6}$$

thus considering only the 2nd quadrant of the dq currents plane, which is indeed the typical range in which an IPMSM is operated (for positive torque). The proper sign of torque will then be actuated by taking it into account in the polar to Cartesian coordinates transformation, i.e. imposing the current references:

$$i_d^* = |i_s^*| \cdot cos(\gamma) \quad , \quad i_q^* = i_s^* \cdot sin(\gamma) \tag{7}$$

In this way, the dependence on the torque sign has been moved from the current space vector phase angle to the q-axis value by considering the already introduced "magnitude with torque sign" i_s^*.

From the mechanical point of view, the drive system will be considered as operating in the neighborhood of a steady-state condition, i.e. at constant speed and subject to a constant load torque. It is worth noticing that the MTPA condition and the definition of current vector angle only make sense for non-null current vector magnitude, i.e. in practice for non-negligible load torque.

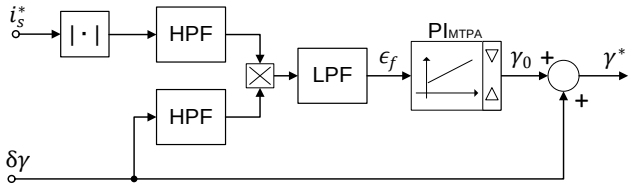

Fig. 3. MTPA tracking loop block diagram.

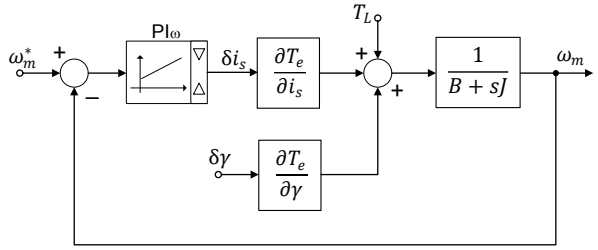

Fig. 4. Small-signal linearized equivalent model of the speed control loop.

III. MTPA Tracking Loop: Dynamics Analysis

Searching for the MTPA point can be described as an optimization problem, [13]. If a certain load condition is considered, in which the machine produces a constant torque T_0, the MTPA condition is found as the current vector angle value γ_{MTPA} that minimizes the current amplitude $|i_s(\gamma)|$:

$$\min_{\gamma} |i_s(\gamma)| \quad \text{subject to} \quad T_e(i_s, \gamma) = T_0 \tag{8}$$

Since the desired minimum is unique in (6), this corresponds to searching for a value γ_{MTPA} which satisfies the condition

$$\frac{di_s}{d\gamma}(\gamma_{MTPA}) = 0 \tag{9}$$

To this purpose, a small oscillating angle signal will be used to test the derivative, in order to obtain a proper current phase angle correction signal. As represented in Fig. 3, the current vector angle reference γ^* is calculated as the sum of the MTPA tracking loop output (operating point γ_0) and a small sinusoidal signal $\delta\gamma$, having frequency f_i and amplitude A.

$$\gamma^* = \gamma_0 + \delta\gamma = \gamma_0 + A\,sin(2\pi f_i\, t) \tag{10}$$

If the injection frequency f_i is much lower than the current control bandwidth, the actual value of the current vector is assumed to be equal to the reference, i.e. $\gamma = \gamma^*$ and $i_s = i_s^*$.

The speed regulator will synthesize a current amplitude variation, in order to reject the disturbance introduced by the injected current phase angle oscillation, i.e.:

$$i_s(\gamma_0 + \delta\gamma) = i_s(\gamma_0) + \delta i_s = i_{s_0} + \delta i_s \tag{11}$$

where i_{s_0}, γ_0 is the considered equilibrium point. Small-signal analysis allows to draw the equivalent block diagram of speed control loop highlighting current space vector phase angle oscillation $\delta\gamma$ and magnitude δi_s, as shown in Fig. 4. The corresponding linearized transfer function can be therefore calculated, i.e.

$$\begin{aligned} W(s) = \frac{\delta i_s(s)}{\delta\gamma(s)} &= -\frac{\partial T_e}{\partial \gamma}\frac{C(s)\,P(s)}{1-[-C(s)\,P(s)]\frac{\partial T_e}{\partial i_s}} \\ &= \frac{\partial i_s}{\partial \gamma}\frac{C(s)P(s)\frac{\partial T_e}{\partial i_s}}{1+C(s)P(s)\frac{\partial T_e}{\partial i_s}} \end{aligned} \tag{12}$$

where $C(s)$ and $P(s)$ are the transfer functions of speed controller and mechanical load plant respectively, while the dynamical part of $W(s)$ corresponds to the closed-loop speed response transfer function $\Omega_{loop}(s)$:

$$\Omega_{loop}(s) = \frac{C(s)P(s)\frac{\partial T_e}{\partial i_s}}{1+C(s)P(s)\frac{\partial T_e}{\partial i_s}} \tag{13}$$

In (12), the equivalence

$$dT_e = \frac{\partial T_e}{\partial i_s}di_s + \frac{\partial T_e}{\partial \gamma}d\gamma = 0 \Rightarrow -\frac{\partial T_e}{\partial \gamma} = \frac{\partial i_s}{\partial \gamma}\cdot\frac{\partial T_e}{\partial i_s} \tag{14}$$

representing a constant-torque condition, has been applied. The derivative $\partial i_s/\partial\gamma$ can be calculated as the ratio:

$$\frac{\partial i_s}{\partial \gamma} = -\frac{i_s\left[\Lambda_{mg}\cos\gamma + (L_d - L_q)i_s\cos 2\gamma\right]}{\sin\gamma\left[\Lambda_{mg} + (L_d - L_q)2i_s\cos\gamma\right]} \tag{15}$$

If the injected phase angle signal $\delta\gamma$ as defined in (10) is considered, the current vector magnitude oscillation δi_s in the time domain at sinusoidal steady-state becomes

$$\begin{aligned} \delta i_s(t) = \frac{\partial i_s}{\partial \gamma}\,&\left|\Omega_{loop}(j2\pi f_i)\right| \\ &\cdot A\,sin\left(2\pi f_i\,t + \angle\{\Omega_{loop}(j2\pi f_i)\}\right) \end{aligned} \tag{16}$$

where $\left|\Omega_{loop}(j2\pi f_i)\right|$ and $\angle\{\Omega_{loop}(j2\pi f_i)\}$ are the magnitude and phase, respectively, of the closed-loop speed control transfer function $W(s)$, calculated at the injection frequency, i.e. with $s = j2\pi f_i$.

As demonstrated in [14], the component of (16) at the injection frequency, once AM-demodulated and low-pass filtered (see also the block diagram in Fig. 3), results in the error signal ϵ_f, which is proportional to the derivative $di_s/d\gamma$, i.e.

$$\begin{aligned} \epsilon_f &= LPF\{\delta i_s \cdot \delta\gamma\} \\ &\approx \frac{1}{2}\,k_{HPF}^2(j2\pi f_i)\,\Re\{\Omega_{loop}(j2\pi f_i)\}\,A^2\,\frac{di_s}{d\gamma} \end{aligned} \tag{17}$$

where $\Re\{\Omega_{loop}(j2\pi f_i)\}$ is the real part of the speed regulation transfer function calculated at the injection frequency.

The high-pass filter on current magnitude (Fig. 3) is required in order to ideally eliminate the effect of the fundamental current, whose components are concentrated around DC, and the same filtering is applied to the injected signal, thus introducing the same phase-shift on both signals. Since it is required that the components around the injection frequency pass through the filter

undistorted, the filter pole must be much smaller than the injection frequency, i.e. $f_{HPF} \ll f_i$. This means that $k_{HPF}^2(j2\pi f_i)$ in (17), which takes into account the gain of both high-pass filters around f_i, can be approximated to unity:

$$\epsilon_f \approx \frac{1}{2}\Re\{\Omega_{loop}(j2\pi f_i)\}\, A^2\, \frac{di_s}{d\gamma} \tag{18}$$

As it can be seen from (17) and (18), if both the injected angle oscillation amplitude A and the speed control loop transfer function at the injection frequency are non-null, ϵ_f becomes zero only when the derivative $di_s/d\gamma$ is zero. Thus, the MTPA angle tracking can be obtained by controlling ϵ_f to zero by means of the Proportional-Integral (PI) regulator $\mathrm{PI_{MTPA}}$ (see Fig. 3), which synthesizes the value of the operating point angle γ_0. As shown in [14], the second derivative $d^2 i_s/d\gamma^2$ is always positive in the whole considered range, confirming that the zero corresponds to a minimum.

IV. MTPA Tracking Loop: Stability Analysis

The gains of $\mathrm{PI_{MTPA}}$ must be chosen properly, in order to achieve stability and a satisfactory convergence rate. In [14], Lyapunov stability condition was derived by using the candidate function

$$V(t) = \frac{1}{2}\epsilon_f^2(t) \tag{19}$$

and considering a purely integral regulator for tracking, i.e.

$$\frac{d\gamma}{dt} = -\epsilon_f K_{i_{MTPA}} \tag{20}$$

Lyapunov derivative can be written as

$$\frac{dV}{dt} = \frac{dV}{d\epsilon_f}\frac{d\epsilon_f}{d\gamma}\frac{d\gamma}{dt} = -K_{i_{MTPA}}\epsilon_f^2\frac{d\epsilon_f}{d\gamma} < 0 \tag{21}$$

Stability was verified only numerically, for any positive integral gain $K_{i_{MTPA}}$, by testing the inequality

$$\frac{d\epsilon_f}{d\gamma} = \frac{d}{d\gamma}\left(\frac{1}{2}A^2\frac{di_s}{d\gamma}\,\Re\{\Omega_{loop}(j2\pi f_i)\}\right) > 0 \tag{22}$$

in many different operating conditions.

In fact, an analytical solution for (22) has not been obtained, due to its complexity. Moreover, its calculation involves speed regulator gains, together with several physical parameters, namely the motor magnetic parameters and the characteristics of the mechanical load, which are all prone to possible inaccuracy. However, some useful considerations will be introduced hereafter about the closed-loop speed control transfer function.

If the injection frequency is chosen so that it lies well within the speed control bandwidth, the closed-loop response can be approximated to unity:

$$\Omega_{loop}(j2\pi f_i) \approx 1 \tag{23}$$

This condition leads to an important simplification of the analysis of the MTPA tracking behavior, as it will be shown in the following. At the same time, according to (18), unitary speed response also ensures the maximum strength of the useful signal for a given injection amplitude.

If the control scheme shown in Fig. 1 is considered, this condition may be more difficult to ensure, due to the current-to-torque characteristics non-linear dependence on the operating point. This effect is locally described by the derivative $\partial T_e/\partial i_s$, as shown in Fig. 4. The adoption of the alternative torque control method represented in Fig. 2 is equivalent to the presence of a speed regulator which compensates for the just mentioned non-linearity, achieving an invariant speed regulation loop behavior. Of course this approximation holds until parametric errors are not excessive. In some applications it may be impractical to extend the speed control bandwidth above a certain value, or motor parameters may be known with strong uncertainty. These conditions may result in an unacceptably low injection frequency limit, in order to ensure (23). In these cases, the use of a resonant term in the speed regulator, centered at the injection frequency (as done in [13] for the current controller), could represent a viable solution.

Application of (23) simplifies both the expression (18)

$$\epsilon_f \approx \frac{1}{2}\, A^2\, \frac{di_s}{d\gamma} \tag{24}$$

and the stability condition (22), which becomes

$$\frac{d\epsilon_f}{d\gamma} = \frac{1}{2}A^2\frac{d^2 i_s}{d\gamma^2} > 0 \tag{25}$$

Since, as already mentioned, it can be shown that the derivative $d^2 i_s/d\gamma^2$ is positive for any $\gamma \in [\pi/2, \pi]$, [14], (25) is verified for the considered angle range.

V. MTPA Tracking Loop: Gain Adaptation and Regulator Design

Beyond demonstrating the stability of the MTPA tracking process, it is also interesting to characterize its dynamics, for the sake of a proper design of the complete drive controller. In [14], an upper bound for the convergence time was also obtained, although by means of a quite complex calculation. However, due to the loop non-linearity, the problem of designing the tracking regulator gains in closed-form, with the aim of achieving predictable dynamics, was not addressed. This is a critical issue especially for general-purpose industrial drives. In fact, in that case motor parameters are not known a priori, but they are typically identified within a self-commissioning procedure, e.g. [5]-[7]. Therefore setting of control parameters is based on the identified machine model, and an auto-tuning procedure for the MTPA tracking gains is actually needed.

The proposal discussed hereafter is based on a local linearization of the loop, considering normal operation as an infinite sequence of steady-state points. Equalization of the dynamics is achieved by on-line adaptation of the loop gain as a function of the operating conditions. Sensitivity analysis is finally considered in order to validate the proposed design and adaptation procedure within actual operating machine conditions, where parameters uncertainty and variations are considered.

A. *Tracking regulator design and stability analysis*

The non-linear tracking loop can be conveniently represented as in Fig. 5. The small-signal equivalent model of the plant is:

$$g \triangleq \frac{d\epsilon_f}{d\gamma} \tag{26}$$

The loop dynamics can be normalized dividing the error signal by an on-line estimate $\hat{g} \approx g$ of the gain, which can be calculated as in (25), exploiting (15):

$$\begin{aligned}\hat{g} &= \frac{1}{2}A^2\frac{\partial^2 i_s}{\partial\gamma^2} \\ &= -\frac{1}{2}A^2\frac{\partial}{\partial\gamma}\left(\frac{i_s\left[\Lambda_{mg}\cos\gamma + \left(L_d - L_q\right)i_s\cos 2\gamma\right]}{\sin\gamma\left[\Lambda_{mg} + \left(L_d - L_q\right)2i_s\cos\gamma\right]}\right) \\ &= -\frac{1}{2}A^2\frac{\partial}{\partial\gamma}\left(\frac{N}{D}\right) = -\frac{1}{2}A^2\cdot\frac{\frac{\partial}{\partial\gamma}N\cdot D - \frac{\partial}{\partial\gamma}D\cdot N}{D^2}\end{aligned} \tag{27}$$

where

$$N = i_s\left[\Lambda_{mg}\cos\gamma + \left(L_d - L_q\right)i_s\cos 2\gamma\right] \tag{28}$$

$$D = \sin\gamma\left[\Lambda_{mg} + \left(L_d - L_q\right)2i_s\cos\gamma\right] \tag{29}$$

After the application of this gain scheduling algorithm, the tracking loop results in a linear system, i.e. a small-signal tracking loop dynamics that does no more depend on the operating point. In fact, considering the linearized system as shown in Fig. 6, which comprises the gain adaptation just introduced, the closed-loop system behaves as a first-order low-pass filter in the neighborhood of any steady-state operating point. The large-signal behavior can be tested for stability by studying the derivative of the Lyapunov candidate function (19):

$$\frac{dV}{dt} = \frac{dV}{d\epsilon_f}\frac{d\epsilon_f}{d\gamma}\frac{d\gamma}{dt} = -\frac{K_{i_{MTPA}}}{\hat{g}}\epsilon_f^2\frac{d\epsilon_f}{d\gamma} < 0 \tag{30}$$

where the regulator dynamics is described by the integral law

$$\frac{d\gamma}{dt} = -\frac{K_{i_{MTPA}}}{\hat{g}}\epsilon_f \tag{31}$$

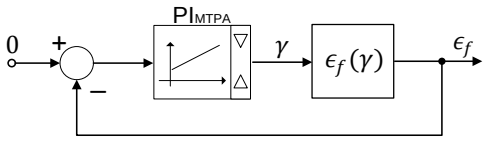

Fig. 5. Equivalent schematic for the tracking loop.

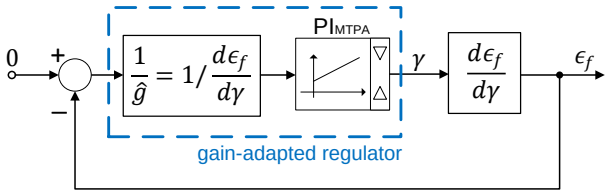

Fig. 6. Equivalent linearized schematic for the derivative-based normalization.

In the case of exact gain normalization according to (26), the inequality (30) is true for any $K_{i_{MTPA}} > 0$:

$$\frac{dV}{dt} = -K_{i_{MTPA}}\epsilon_f^2 < 0 \tag{32}$$

It is worth noticing that, by applying the proposed normalization, the closed-loop dynamics becomes linear in terms of the error signal ϵ_f, which means that the estimated MTPA angle γ will not follow the same dynamics, being non-linearly related to ϵ_f. However, since the error signal reaches zero when γ reaches the MTPA value, the angle convergence time will be similar to that of ϵ_f.

Once the subsystem consisting in the plant and feedback model has been linearized by means of gain normalization, analytical design of the tracking regulator becomes straightforward. Since the open-loop transfer function corresponds to an integrator, its cross-over frequency is equal to the integral gain and also corresponds to the closed-loop bandwidth:

$$K_{i_{MTPA}} = 2\pi\, B_{MTPA} \tag{33}$$

The tracking bandwidth (in Hz), B_{MTPA}, represents the only specification (i.e. the design goal), and is upper limited by the demodulation low-pass filter pole frequency. This in turn needs to be lower than the injection frequency, which should be comprised within the speed control bandwidth, in accordance to previous hypotheses.

The presence of a low-pass filter on the demodulated signal has been disregarded in the previous analysis, since the filter pole (first--order filter has been applied) has to be sufficiently higher than the tracking bandwidth (i.e. between B_{MTPA} and f_i). Also a proportional action could be added in order to speed up the response, [14], but proper gain margins must considered in that case.

As suggested by simple considerations on the small-signal model (then confirmed by simulations), the fundamental current components result in disturbance on the error signal, especially during torque transients, since fundamental current is usually much larger than the injection-related signal. The MTPA tracking loop gain must then have a sufficiently large attenuation at the injection frequency, and at the same time the fundamental current must have little content at the injection frequency. The choice of a proper value for f_i must then be related to the speed regulation bandwidth and desired MTPA tracking dynamics. In fact, a faster speed control *allows* a higher injection frequency to be adopted while keeping approximation (23) valid. On the other hand, a more dynamic speed regulator generates larger and higher-order harmonic components in the current magnitude i_s^* during transients, thus *requiring* a higher injection frequency to be chosen for achieving a sufficient separation between fundamental-related and injection-related frequency components. If particularly wide MTPA tracking bandwidth is desired (or very small signal is injected), it may be difficult to achieve this simply by proper design of the first-order low-pass and high-pass filters. In such a case, or in general for better noise reduction, a more selective filter (e.g. notch at the injection frequency) can be added after demodulation.

In general, an interesting result of the proposed approach is that, once a proper configuration has been found and tested for one case (such as in the laboratory experiments reported in this paper),

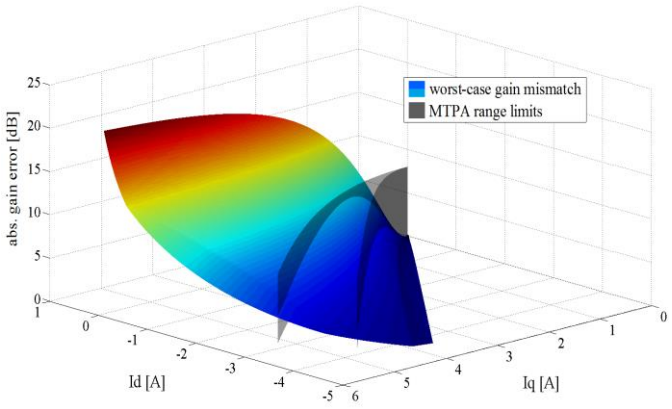

Fig. 7. Worst-case gain variation related to ±25% parameters mismatch.

then it should be possible to change all bandwidth values (speed control, low-pass filtering and MTPA tracking) and injection frequency accordingly, i.e. keeping the same ratios between them. This should result in a similar behavior (but with scaled dynamics), for any motor and in the whole operating range. The upper limit for bandwidth is of course imposed by the current control, as already pointed out. The application of any design rule, comprising the more complex ones and those involving the use of advanced tools, becomes also possible thanks to the proposed gain adaptation.

B. Sensitivity analysis

From the previous sub-section it may *appear* that the exact knowledge of machine parameters is crucial for the application of the method, since parameters are involved in the gain compensation. If this were strictly true, such an MTPA tracking technique would be almost useless, since its main purpose is to overcome parametric uncertainty. However, a *coarse knowledge* of the motor parameters is sufficient for linearization of the tracking loop dynamics. In fact, a limited gain error just modifies the algorithm convergence rate, leaving steady-state result unaffected. This can only become critical if adaptation factor results in the wrong sign, but this condition can be avoided by properly saturating $\hat{g}$, since this quantity is expected to be always positive in the considered range of γ. With limited normalization error, stability can be still ensured if sufficient margins have been adopted.

The effect of gain adaptation error was investigated for the machine considered in simulation and experiments. To this purpose, the effect of mismatch of motor magnetic parameters (L_d, L_q, Λ_{mg}) on the calculated gain has been analyzed numerically. Under the hypothesis of ±25% mismatch with respect to nominal values, all the possible combinations of parametric errors have been considered (i.e. +25% and -25% difference on all the three values). The gain has then been calculated, according to (27), both for the supposed (i.e. nominal) and actual (mismatched) parameter values.

The absolute value of gain mismatch (in dB), i.e. the ratio between supposed and actual gain, has been evaluated and for each point of calculation the worst-case (i.e. maximum difference) has been represented using the colored surface in Fig. 7.

The evaluation domain was limited to the range in which, given ±25% parameters variation, MTPA could lie, i.e. where MTPA tracking will realistically take place (delimited by grey walls in Fig. 7). For the motor considered in this paper, as it can be seen in Fig. 7, even quite large parameter tolerance (±25%) can lead to maximum ±7 dB mismatch between expected and actual gain in the selected area. This means that the resulting dynamics due to erroneous normalization can be slightly more than twice as faster or twice as slower with respect to the design target.

VI. Simulation Results

The whole drive system has been simulated in the Matlab/Simulink environment, implementing the machine model in continuous-time and the controller one in sampled-time. A prototype 2.2 kW IPM motor has been considered, whose rated parameters are listed in Table I. Results confirmed the feasibility

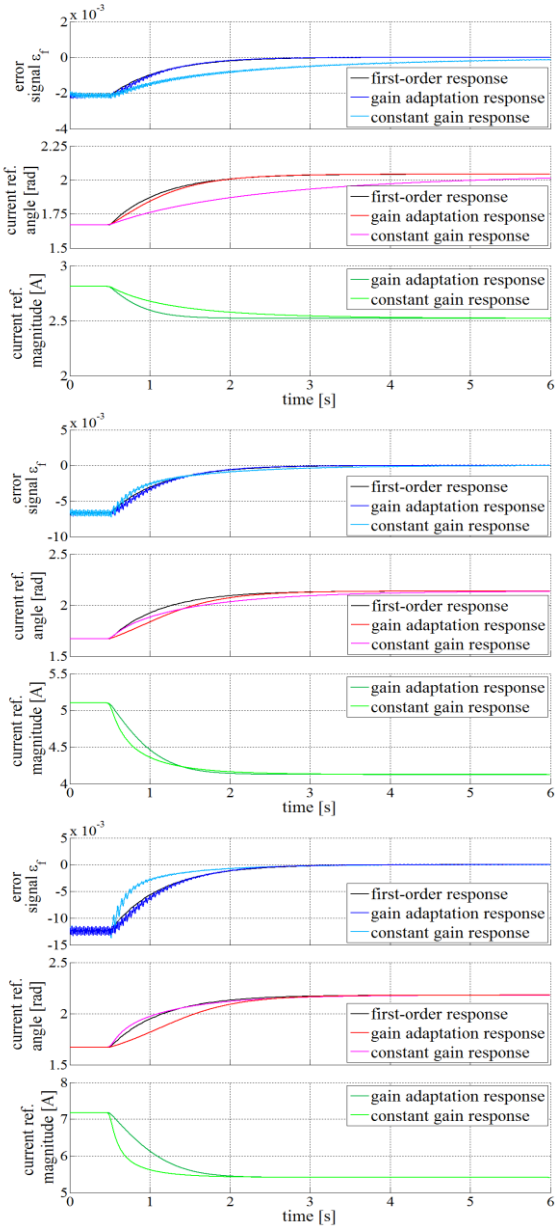

Fig. 8. MTPA tracking algorithm with and without gain adaptation: simulated step response test at 500rpm, load torque is 2, 4 and 6 Nm (from top to bottom respectively), injected signal is 50 mrad at 20 Hz.

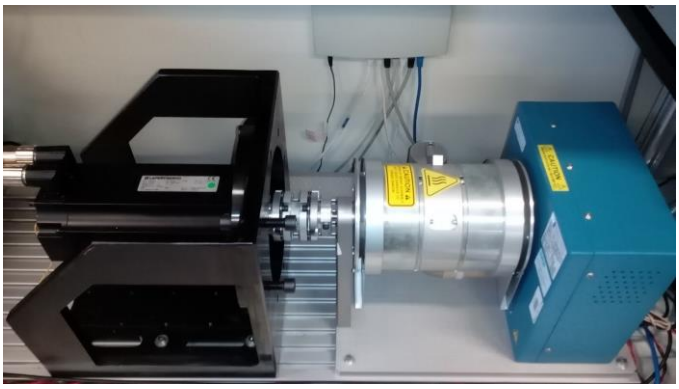

Fig. 9. Experimental test bench.

of the proposal, and highlighted some important implementation details to be taken into account.

Fig. 8 aims at showing the response of the MTPA tracking loop under different conditions, comparing the cases with and without gain adaptation The step response is reported in Fig. 8 for the cases of 2, 4 and 6 Nm load (from top to bottom, respectively) at 500 rpm constant speed. Injection is performed at 20 Hz frequency and 50 mrad (about 2.9 degrees) amplitude. The tracking algorithm is enabled at 500 ms with initial value $\gamma^* = \pi/2 + A$ rad (where A is the injection amplitude), and the tracking bandwidth is set to 0.25 Hz. The top subplot shows the error signal ϵ_f, while in the second diagram the current vector angle reference γ^* is reported. In both cases a corresponding first-order response is shown, in order to compare the actual dynamics to the design target, i.e. first-order 0.25 Hz closed-loop response bandwidth. The bottom subplot shows the current reference amplitude, which is considerably reduced when the algorithm is activated.

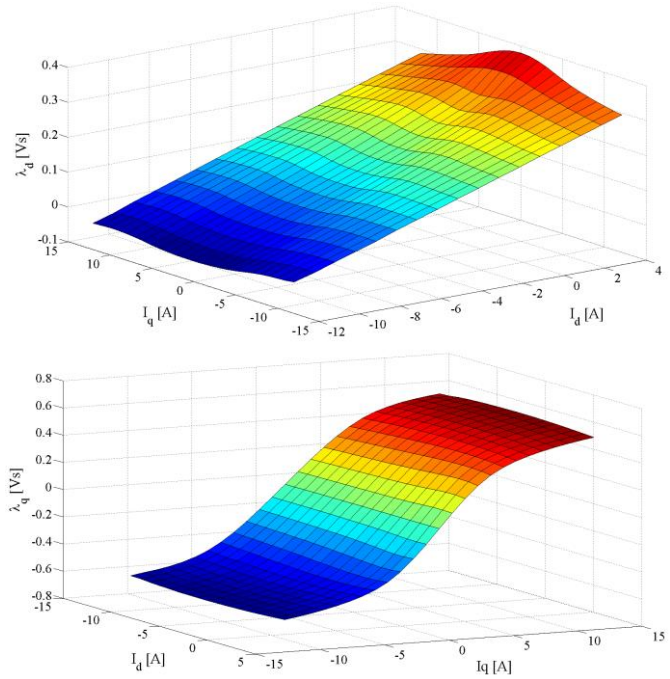

Fig. 10. Flux-linkage maps for the d-axis (top) and q-axis (bottom).

It can be clearly seen that, when gain adaptation according to the schematic in Fig. 6 is adopted, the error signal closely follows the designed first-order dynamics in all the three load conditions. On the other hand, the current reference angle is close to the first-order trace for the lowest torque value (2 Nm), while it becomes increasingly different in the other two cases. As discussed in section V, this is explained by the increasing non-linearity of the loop, since the gain adaptation results in a first-order response *for the error signal*, while the angle settles around the MTPA value in the same time, but with a different trend. It is also worth noticing that the reduction in current amplitude also follows approximately the designed first-order behavior.

The results related to fixed-gain behavior have been obtained under similar conditions, in order to show the effect of plant gain variations. In this case the integral gain has been chosen considering an objective tracking bandwidth of approximately 0.25 Hz at medium load torque. The resulting dynamics becomes considerably different between the maximum and minimum load torque cases (i.e. 6 Nm vs. 2 Nm), in fact the rise time of the error signal ϵ_f is about 1.1 s in the high-torque case (approximately 0.3 Hz bandwidth), while it is 4.5 s in the low-torque test (about 0.08 Hz bandwidth). It is worth remarking that, despite gain adaptation was not adopted in this case, the analytical approach to the study of dynamics was still useful, since evaluating the static gain of the plant at a certain operating point (e.g. nominal torque in MTPA, or a medium-current and intermediate angle condition) has been exploited in the choice of an acceptable value for the regulator gain, avoiding time-consuming trial-and-error tuning. This possibility also confirms the usefulness of the proposed analysis.

VII. Experimental Results

The proposed control algorithm has been implemented on the hardware of a Gefran ADL-200 5.5kW commercial drive. With respect to a drive coming from the normal production line, the only modifications introduced concern part of the motor control algorithm. The proposed algorithm is thus fully suitable to deployment in real-world applications, on standard hardware architectures. The digital control board is based on a microcontroller of the Infineon Tricore family, running at 75 MHz, which also carries out the tasks of communication, parameter exchange management and execution of user-customizable PLC code. Sampling and switching frequency are both 10 kHz. With the present implementation the execution of all the IPMSM speed control algorithm (including the proposed method and update of output variables used for display and debugging purposes) lasts less than half of the control cycle (i.e. less than 50 µs).

Both dynamics and steady-state accuracy of the method have been tested for the same machine considered in the simulations. The laboratory test bench comprises a Magtrol HD-715 hysteresis brake with high- accuracy torque measurement and control, which is coupled to the motor under test, Fig. 9. Despite the presence of magnetic saturation (see Fig. 10), [5][7], constant self-identified motor parameters were used both for the design of controllers, torque control (according to the schematic in Fig. 2) and MTPA gain adaptation, resembling the case of a real-world situation in which MTPA tracking would be needed (i.e. when complete flux-linkage maps are not available).

Fig. 11 shows the step response of the MTPA tracking loop in the same conditions considered in Fig. 8, *with* gain adaptation. For the three load torque values (2, 4 and 6 Nm), the dynamical response is in very good agreement with the theoretical and simulation results, although a relatively large low-frequency oscillation (at 3.3 Hz) is present on the error signal ϵ_f. The different value of current magnitude between simulation and experiments in the 6 Nm test (especially in the initial condition, i.e. far from the MTPA) is due to the fact that magnetic saturation was neglected in the simulation model, while it is actually not negligible for large q-axis current (see Fig. 10). The propagation of low-frequency oscillations to the estimated MTPA angle at steady-state is certainly undesirable, since it results in slightly increased acoustic noise, losses and torque ripple.

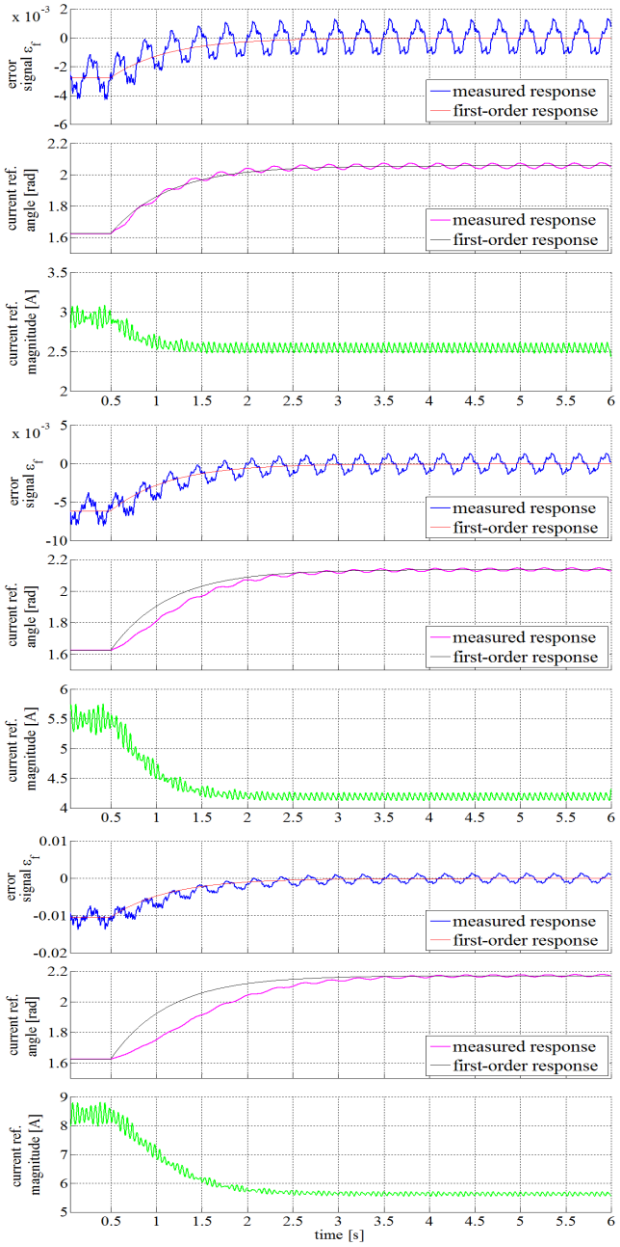

Fig. 11. Proposed MTPA tracking algorithm (0.25 Hz bandwidth): experimental step response test at 500rpm, load torque is 2, 4 and 6 Nm (from top to bottom respectively), injected signal is 50 mrad at 20 Hz.

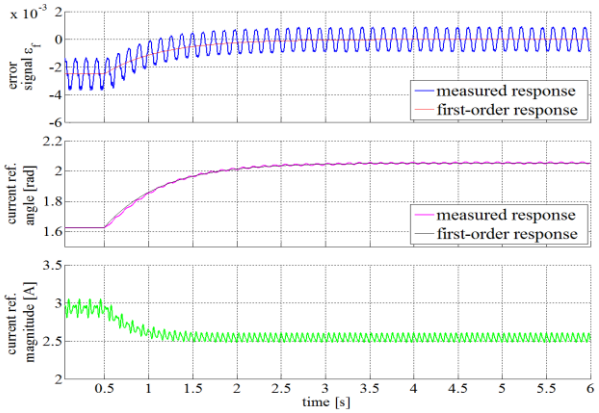

Fig. 12. MTPA tracking step response, all parameters as in Fig. 11 (top), except injection frequency is 25 Hz.

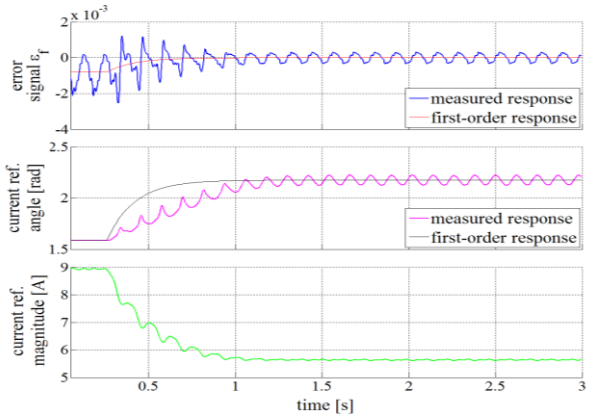

Fig. 13. MTPA tracking step response, test conditions as in Fig. 11 (bottom), injected signal is 12.5 mrad at 25 Hz, design tracking bandwidth is 1 Hz.

By simple reasoning, it is possible to attribute this effect to the presence of a non-negligible harmonic of the current magnitude at the electrical frequency ($f_{el} = 16.7$ Hz). In fact, if a component of measured current magnitude δi_s at a certain frequency f is demodulated together with the useful signal, it results, after processing, in harmonics at the difference and sum between the original component f and the injection (and demodulation) carrier frequency. If a disturbance at the electrical frequency f_{el} is present (which may be caused by current measurement DC offset and subsequent Park transformation), the demodulation results in a disturbance at $f_i - f_{el}$ and $f_i + f_{el}$. The component at $f_i + f_{el}$ corresponds, in the first case (Fig. 12), to 20+16.67 = 26.67 Hz, and is almost eliminated by low-pass filtering, while the one at $f_i - f_{el}$ = 3.3 Hz is not sufficiently attenuated and is the one clearly visible in the results.

In order to prove the correctness of this consideration and to address the related issue, a further test has been performed at the same speed and at 2 Nm load (where the oscillations are more visible), but with a different injection frequency (25 Hz). In this case (Fig. 12), the disturbance appears at 8.33 Hz, (mainly visible on the error signal), and its effect on the estimated angle is attenuated so that it becomes hardly visible in the diagram. More in general, mechanical and/or electrical non-ideal behavior could result in harmonic disturbance of the estimated MTPA angle. To reduce the influence of these

effects, the injection frequency could be changed depending on speed, in order to keep integer harmonics of the mechanical frequency out of the band of interest, i.e. far from the carrier.

In order to test the method in "extreme" conditions, a test similar to that in Fig. 11 (bottom) has been carried out (i.e. the ones shown in Fig. 13). Successful tracking operation is demonstrated even with four-fold bandwidth (1 Hz) and injected signal amplitude decreased to one-fourth (i.e. 12.5 mrad, or about 0.7 deg), with respect to previous experiments. Although undesired oscillations are more relevant due to the lower signal-to-noise ratio, stable behavior is obtained and the dynamics is compatible with the design specification. The choice of the injection signal strength still represents an open point, since the optimum mainly depends on the noise level. It is worth noticing that the same problem arises in most cases where signal injection is applied (i.e. especially in saliency-based sensorless position and speed estimation), where this choice is typically done by trial-and-error. It is reasonable to consider current measurement non-ideality to be one of the main sources of noise, thus the amplitude should at least scale according to the full-scale value of the current measurement in the drive system. Then it can be predicted that, once a good compromise has been obtained for a certain drive size, signal amplitude should be scaled with the inverter current rating.

The accuracy of MTPA tracking is analyzed in Fig. 14. Current space vector magnitude values for different angles are shown in the left diagram (empty circles), as a result of steady-state measurements at 2, 4 and 6 Nm load torque. Actual MTPA points are marked as filled circles with black contour. The same points are also reported in the synchronous plane (diagram on the right) together with current trajectories followed during the step response tests considered in Fig. 11. The MTPA curves obtained using data from different characterization techniques are also shown for comparison. The yellow trace represents the analytical curve resulting from linear approximation of the flux maps (i.e. constant inductances), the light blue one is obtained from numerical processing of the motor flux LUTs (maps in Fig. 10), while the magenta curve is based on the flux characteristics identified according to [5] (linear + saturation approximating curve). Considering the entire diagram, it can be concluded that the MTPA tracking algorithm achieves good accuracy, since the final values overlap the actual MTPA points (circles), while small differences with respect to the flux map based curve exist. In general, small discrepancies can be explained by measurement noise, quantization of flux-linkage acquisition and temperature variations (which mainly act on the permanent magnet flux-linkage). In fact, very small current magnitude differences exist between points in the neighborhood of the MTPA loci, for the same torque.

Finally, Fig. 15 shows an experiment which has been performed in order to test the MTPA tracking controller in a challenging condition, i.e. during a constant speed control at 300 rpm under a sudden increase of the load torque from 0 to 6 Nm and back to no-load. Injection frequency is set to 30 Hz. It can be seen that the MTPA tracking loop correctly activates and settles to the steady-state value, with a dynamical behavior which is very similar to that of Fig. 11 (bottom). The tracking is disabled when current is below 0.5 A, causing the abrupt decrease of angle at 4.75 s. Looking at the error signal trace it is possible to notice increased oscillations corresponding to the load transients. This behavior can be explained considering that fast variations of the torque request (i_s^*) by the speed regulator lead to the presence of relatively high-frequency components of the current magnitude signal i_s. As already mentioned in section V.A, those components lying in the band around the injection frequency will be seen as noise by the MTPA tracking loop.

However, the experiment confirms the robustness of the method even in the presence of relatively fast torque transients, leading to the conclusion that a proper choice of the MTPA tracking bandwidth allows reliable speed control. Implementation of a complex enable/disable logic (as in [10]) is not strictly required, but could be considered when MTPA tracking is to be applied to very wide-bandwidth speed control (e.g. servo applications). In those cases, MTPA tracking during fast transients could also be improved both by designing a wider bandwidth regulation loop and/or introducing a feed-forward based on a conventional MTPA implementation so that the feedback acts as a fine-tuning (as proposed in [9]). For achieving proper operation of the system in the entire speed range, during flux-weakening the signal injection should be disabled and the MTPA tracking regulator locked.

Some applications could also benefit from MTPA tracking as part of a self-commissioning procedure, in order to detect the actual MTPA trajectory to be stored in Look-Up Tables or approximating functions, for use during the normal operation. This would allow, for example, to fully exploit the torque density of an IPMSM without the need for very accurate self-identification algorithms.

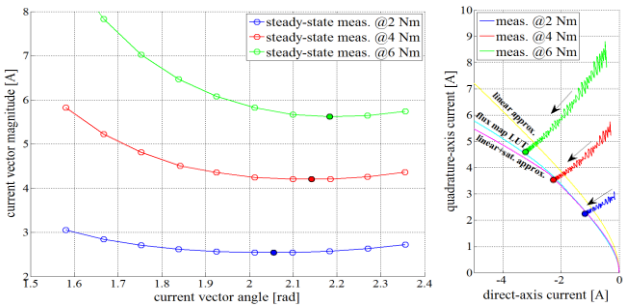

Fig. 14. Steady-state current space vector magnitude vs. angle under different load values (left) and dynamical trajectories in the dq current plane (right).

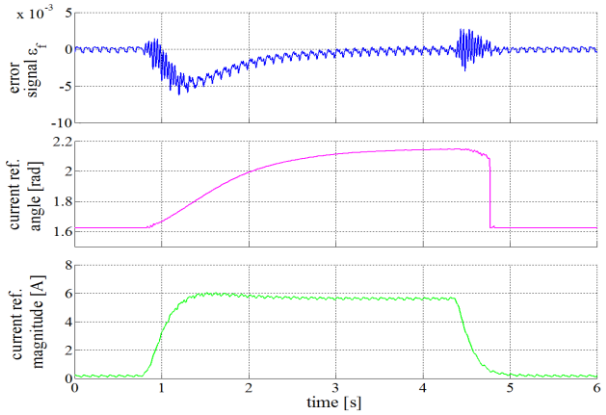

Fig. 15. MTPA tracking operation during 6 Nm load torque transient.

VIII. CONCLUSIONS

Automatic MTPA tracking based on extremum seeking through signal injection has been considered in this paper. Design of the tracking loop dynamics represents the main topic and the original contribution of this paper, which was never reported in past literature.

A recent and efficient MTPA tracking method based on signal injection has been considered for the analysis and as a case study. Most of the proposed ideas, design approach and adaptation strategy are indeed general and can be extended to any control scheme implementing closed-loop MTPA tracking.

Calculation of the non-linear small signal gain of the tracking loop has been achieved in closed form, leading to two valuable results:

- dynamics can be programmed for each operating point by optimal design of the tracking regulator;
- on-line adaptation can be applied, making the designed MTPA tracking loop dynamics invariant with the operating point.

Leveraging the proposed analysis, it has been shown that a simple yet reliable design rule can be applied, which allows to obtain a first-order MTPA tracking loop response with the desired bandwidth, independent of the operating condition. The design procedure is also suitable for auto-tuning and allows on-line adaptation of the tracking regulator in order to normalize the loop transfer function, making the MTPA tracking dynamics invariant with the operating point. The computational burden related to on-line adaptation is limited and absolutely acceptable for a typical drive control system.

Complementary topics have also been considered, aiming at evaluating the performances of the proposed design approach on an actual application scenario, i.e.:

- the influence of any parametric error (which may be due to identification inaccuracy or parameter variation) on the tracking dynamics;
- stability analysis of the closed-loop tracking loop, based on Lyapunov approach;
- the effect of DC current measurement offset on the steady-state output ripple of the tracking loop.

Experimental implementation has been carried out based on a commercial (Gefran ADL-200 5.5kW) drive hardware. The feasibility and effectiveness of the method has been tested considering a typical application scenario, i.e. using constant self-identified parameter values.

Although the MTPA tracking approach is meant to be applied in quasi-steady-state conditions, robust and stable operation was demonstrated also with varying load, making the method suitable for any application requiring a certain degree of accuracy of operation within the MTPA locus of the machine. Parametric and stability analysis proved that accurate and stable response of the tracking loop is assured in any operating condition, allowing interior permanent magnet (and potentially also to synchronous reluctance) motor drives to maximize their torque-to-current performance even in the case of inaccurate knowledge of machine parameters.

TABLE I. RATED PARAMETERS OF IPMSM

Torque	6.7	$[Nm]$
Speed	3000	$[rpm]$
Voltage (*phase-to-phase*)	330	$[V_{rms}]$
Current	4.2	$[A_{rms}]$
Pole pairs	2	
d-axis inductance	22	$[mH]$
q-axis inductance	95	$[mH]$
PM flux linkage	0.237	$[Vs]$

IX. REFERENCES

[1] T.M. Jahns, G.B. Kliman, and T.W. Neumann, "Interior Permanent-Magnet Synchronous Motors for Adjustable-Speed Drives," *IEEE Trans. on Industry Applications*, vol. 22, no. 4, pp. 738–747, July 1986.

[2] H.B. Kim, H. Hartwig, and R.D. Lorenz, "Using on-line parameter estimation to improve efficiency of IPM machine drives," in *Proc. of the 33rd IEEE Power Electronics Specialists Conf.*, vol. 2, pp. 815-820, 2002.

[3] Y.A.-R.I. Mohamed, and T.K. Lee, "Adaptive Self-Tuning MTPA Vector Controller for IPMSM Drive System," *IEEE Trans. on Energy Conversion*, vol. 21, no. 3, pp. 636-644, Sept. 2006.

[4] S. J. Underwood, and I. Husain, "Online Parameter Estimation and Adaptive Control of Permanent-Magnet Synchronous Machines," *IEEE Trans. on Industrial Electronics*, vol. 57, no. 7, pp. 2435-2443, July 2010.

[5] N. Bedetti, S. Calligaro, and R. Petrella, "Stand-still Self-Identification of Flux Characteristics for SynRM using Novel Saturation Approximating Function and Multiple Linear Regression," in *Prof. of IEEE Energy Conversion Congress and Exposition*, 20-24 Sept., pp. 2995–3002, Montreal, Canada, 2015.

[6] G. Pellegrino, B. Boazzo, and T. M. Jahns, "Magnetic Model Self-Identification for PM Synchronous Machine Drives," *IEEE Trans. on Industry Applications*, vol. 51, no. 3, pp. 2246–2254, 2015.

[7] N. Bedetti, S. Calligaro, and R. Petrella, "Stand-Still Self-Identification of Flux Characteristics for Synchronous Reluctance Machines Using Novel Saturation Approximating Function and Multiple Linear Regression," *IEEE Trans. on Industry Applications*, vol. 52, no. 4, pp. 3083-3092, 2016.

[8] D. Anton, K. Young-Kwan, L. Sang-Joon, and L. Sang-Taek, "Robust self-tuning MTPA algorithm for IPMSM drives," in *Proc. of the 34th IEEE Industrial Electronics Annual Conference*, Orlando, Florida, USA, pp. 1355–1360, 2008.

[9] S. Bolognani, R. Petrella, A. Prearo, and L. Sgarbossa, "Automatic tracking of MTPA trajectory in IPM motor drives based on AC current injection," *IEEE Trans. on Industry Applications*, vol. 47, no. 1, pp. 105-114, Jan.-Feb. 2011.

[10] S. Bolognani, R. Petrella, A. Prearo, and L. Sgarbossa, "On-line tracking of the MTPA trajectory in IPM motors via active power measurement," in *Proc. of XIX Int. Conference on Electrical Machines*, Rome, Italy, 2010.

[11] S. Kim, Y.-D. Yoon, S.-K. Sul, K. Ide, and K. Tomita, "Parameter independent maximum torque per ampere (MTPA) control of IPM machine based on signal injection," in *25th IEEE Applied Power Electronics Conference and Exposition*, 21-25 February, pp. 103-108, Palm Springs, California, USA, 2010.

[12] S. Bolognani, L. Peretti, and M. Zigliotto, "Online MTPA Control Strategy for DTC Synchronous-Reluctance-Motor Drives", *IEEE Trans. on Power Electronics*, vol. 26, no. 1, pp. 20–28, Jan. 2011.

[13] S. Kim, Y.-D. Yoon, S.-K. Sul, and K. Ide, "Maximum Torque per Ampere (MTPA) Control of an IPM Machine Based on Signal Injection Considering Inductance Saturation," *IEEE Trans. on Power Electronics*, vol. 28, no. 1, pp. 488–497, Jan. 2013.

[14] R. Antonello, M. Carraro, and M. Zigliotto, "Maximum-Torque-Per-Ampere Operation of Anisotropic Synchronous Permanent-Magnet Motors Based on Extremum Seeking Control," *IEEE Trans. on Industrial Electronics*, vol. 61, no. 9, pp. 5086–5093, Sept. 2014.

[15] C. Mademlis and V. G. Agelidis, "A high-performance vector controlled interior PM synchronous motor drive with extended speed range capability," in *Proc. of the 27th Annual Conf. of the IEEE Industrial Electronics Society*, vol. 2, pp. 1475–1482, 2001.

[16] S. Bolognani, S. Calligaro, and R. Petrella, "Adaptive Flux-Weakening Controller for Interior Permanent Magnet Synchronous Motor Drives," *IEEE Journal of Emerging and Selected Topics in Power Electronics*, vol. 2, no. 2, pp. 236–248, June 2014.

[17] S. Calligaro, C. Olsen, R. Petrella, and N. Bedetti, "Automatic MTPA tracking in IPMSM drives: Loop dynamics, design and auto-tuning," in Proc. 2016 IEEE Energy Conversion Congress and Exposition (ECCE), Milwaukee, WI USA, pp. 1 - 8, DOI: 10.1109/ECCE.2016.7854891.